Journal of Visualized Experiments

Morphological and Functional Evaluation of Ribbon Synapses at Specific Frequency Regions of the Mouse Cochlea

--Manuscript Draft--

Article Type:	Invited Methods Article - JoVE Produced Video
Manuscript Number:	JoVE59189R2
Full Title:	Morphological and Functional Evaluation of Ribbon Synapses at Specific Frequency Regions of the Mouse Cochlea
Keywords:	ribbon synapse; cochlear place-frequency map; cochleogram; synaptopathy; CtBP2; GluR2; ABR threshold; ABR wave I amplitudes
Corresponding Author:	Shukui Yu Capital Medical University Affiliated Beijing Friendship Hospital Beijing, Beijing CHINA
Corresponding Author's Institution:	Capital Medical University Affiliated Beijing Friendship Hospital
Corresponding Author E-Mail:	ysy790418@163.com
Order of Authors:	Shukui Yu
	Zhengde Du
	Qingling Song
	Tengfei Qu
	Yue Qi
	Wei Xiong
	Lu He
	Wei Wei
	Shusheng Gong
	Ke Liu
Additional Information:	
Question	**Response**
Please indicate whether this article will be Standard Access or Open Access.	Standard Access (US$2,400)
Please indicate the **city, state/province, and country** where this article will be **filmed**. Please do not use abbreviations.	Beijing, China

September 30, 2018, Beijing, China

Avital Braiman
Editor-in-Chief
Journal of Visualized Experiments

Dear Editor:

I have finished the manuscript according to the requirements of invitation letter and wish to submit this original paper for publication in *Journal of Visualized Experiments*, titled "**Morphological and Functional Evaluation of Ribbon Synapse at Specific Frequency Region of the Mouse Cochlea**." The paper was coauthored by Shu-Kui Yu, Zheng-De Du, Qing-Ling Song, Teng-Fei Qu, Yue Qi, Wei Xiong, Lu He, Wei Wei, Ke Liu, Shu-Sheng Gong.

This manuscript presents a protocol to analyze cochlear synaptic morphology and function at specific frequency region in adult mice. After cochlear frequency localization performed by the combination of the place-frequency map and cochleogram, the morphological characteristic of ribbon synapses is evaluated by synaptic immunostaining and the functional status of ribbon synapses is investigated by amplitudes of ABR wave I. We believe that our protocol can be used as a valuable tool to help deeper understanding the pathological appearances of synaptic dysfunction, exploring their mechanisms, and evaluating the efficacy of a possible therapeutic intervention for future investigations.

Further, we believe that this paper will be of interest to the readership of your journal because we provide detailed and complete descriptions and critical steps for experimental manipulation based on our experience. By above experimental strategy, our lab investigate the number and function of synaptic ribbons in cochlea of normal mice, and find that maximal number of pre-synaptic ribbons is formed in the cochlear region of middle frequency coupling with the lowest ABR threshold and highest CAP amplitudes, suggesting that the middle frequency (8–16 kHz) may be the most sensitive region to sound stimuli in mice. These results have been published in our latest article in *Acta Oto-Laryngologica*, titled "**Maximal number of pre-synaptic ribbons are formed in cochlear region corresponding to middle frequency in mice**."

The experimental protocol presented in this paper has been used to generate data previously published in other journals. But the content including representative results and figures in this original manuscript does not overlap with any other previously published article by us. A majority of methods used in this paper have also been improved upon following original use, all of which are the most recent version for this submission. We have read and understood your journal's policies, and we believe that neither the manuscript nor the study violates any of these. There are no conflicts of interest to declare.

Thank you for your consideration. I look forward to hearing from you.

Sincerely,
Ke Liu
Department of Otolaryngology - Head and neck surgery, Beijing Friendship Hospital, Capital Medical University, 95 Yong An Road, Beijing, 100050, China.
E-mail: Keliu66@hotmail.com
Tel: +86 13811488642

TITLE:

Morphological and Functional Evaluation of Ribbon Synapses at Specific Frequency Regions of the Mouse Cochlea

AUTHORS & AFFILIATIONS:

Shu-Kui Yu[1]*, Zheng-De Du[1]*, Qing-Ling Song[1], Teng-Fei Qu[1], Yue Qi[1], Wei Xiong[1], Lu He[1], Wei Wei[2], Shu-Sheng Gong[1], Ke Liu[1]

[1]Department of Otolaryngology-Head and Neck Surgery, Beijing Friendship Hospital, Capital Medical University, Beijing, China

[2]Department of Otology, Shengjing Hospital of China Medical University, Shenyang, China

*These authors equally contributed to this work.

Corresponding Authors:

Ke Liu (Keliu66@hotmail.com)

Shu-Sheng Gong (gongss1962@163.com)

Email Addresses of Co-authors:

Zhengde Du (duzhengde@163.com)

Qingling Song (402315133@qq.com)

Tengfei Qu (qutengfei812@126.com)

Yue Qi (qi_yueqiyue@126.com)

Wei Xiong (18710180715@139.com)

Lu He (Drhelu@126.com)

Wei Wei (ydvv14@163.com)

Shusheng Gong (gongss1962@163.com)

Ke Liu (Keliu66@hotmail.com)

KEYWORDS:

Ribbon synapse, cochlear place-frequency map, cochleogram, synaptopathy, CtBP2, GluR2, ABR threshold, ABR wave I amplitudes

SUMMARY:

This manuscript describes an experimental protocol for evaluating the morphological characteristics and functional status of ribbon synapses in normal mice. The present model is also suitable for noise-induced and age-related cochlear synaptopathy-restricted models. The correlative results of previous mouse studies are also discussed.

ABSTRACT:

Cochlear inner hair cells (IHCs) transmit acoustic signals to spiral ganglion neurons (SGNs) through ribbon synapses. Several experimental studies have indicated that hair cell synapses may be the initial targets in sensorineural hearing loss (SNHL). Such studies have proposed the concept of cochlear “synaptopathy”, which refers to alterations in ribbon synapse number, structure, or function that result in abnormal synaptic transmission between IHCs and SGNs. While cochlear

synaptopathy is irreversible, it does not affect the hearing threshold. In noise-induced experimental models, restricted damage to IHC synapses in select frequency regions is employed to identify the environmental factors that specifically cause synaptopathy, as well as the physiological consequences of disturbing this inner ear circuit. Here, we present a protocol for analyzing cochlear synaptic morphology and function at a specific frequency region in adult mice. In this protocol, cochlear localization of specific frequency regions is performed using place-frequency maps in conjunction with cochleogram data, following which the morphological characteristics of ribbon synapses are evaluated via synaptic immunostaining. The functional status of ribbon synapses is then determined based on the amplitudes of auditory brainstem response (ABR) wave I. The present report demonstrates that this approach can be used to deepen our understanding of the pathogenesis and mechanisms of synaptic dysfunction in the cochlea, which may aid in the development of novel therapeutic interventions.

INTRODUCTION:

Frequencies in the range of approximately 20–20,000 Hz can be perceived as auditory stimuli by humans. Human hearing is normally most sensitive near 1,000 Hz, where average sound pressure level is 20 µPa in young adults (i.e., 0 decibels of sound pressure level [dB SPL]). In some pathological conditions, hearing loss is restricted to specific frequencies. For example, in the early stages of noise-induced hearing loss (NIHL), a "notch" (i.e., hearing threshold elevation) can be observed in the audiogram at 4 kHz[1]. Along the mammalian cochlear partition, its gradations of stiffness and mass produce an exponential frequency map, with high-frequency sound detection at the base of the cochlea and low-frequency detection at the apex[2]. Indeed, there is a cochlear place-frequency map along the basilar membrane, leading to what is known as tonotopic organization[2,3]. Each given place on the basilar membrane has the highest sensitivity to only one particular sound frequency, which is usually termed the characteristic frequency[3,4], although responses to other frequencies can also be observed.

To date, various mouse models have been employed to investigate normal function, pathological processes, and therapeutic efficacy in the auditory system. Precise knowledge of physiological parameters in the mouse cochlea is a prerequisite for such studies of hearing loss. The mouse cochlea is anatomically divided into apical, middle, and basal turns, which correspond to different frequency regions. By labeling auditory nerve afferents at the cochlear nucleus to analyze their corresponding peripheral innervation sites in the cochlea, Müller et al. succeeded in establishing the cochlear place-frequency map in the normal mouse in vivo[5]. In the interval of 7.2–61.8 kHz, which corresponds to positions between 90% and 10% of the full length of the basilar membrane, the mouse cochlear place-frequency map can be described by a simple linear regression function, suggesting a relation between the normalized distance from the cochlear base and the logarithm of the characteristic frequency[5]. In laboratory mice, the place-frequency map can be used to explore the relationship between hearing thresholds within specific frequency ranges and cochleograms showing the numbers of missing hair cells in relative regions along the basilar membrane[6]. Importantly, the place-frequency map provides a positioning system for the investigation of minimal structural damage, such as damage to the ribbon synapses of hair cells at specific cochlear frequency locations in mice with peripheral auditory trauma[7,8].

In the mammalian cochlea, ribbon synapses are comprised of a presynaptic ribbon, an electron-dense projection that tethers a halo of release-ready synaptic vesicles containing glutamate within the IHC, and a postsynaptic density on the nerve terminal of the SGN with glutamate receptors[9]. During cochlear sound transduction, deflection of the hair cell bundle results in IHC depolarization, which leads to glutamate release from IHCs onto the postsynaptic afferent terminals, thereby activating the auditory pathway. Activation of this pathway leads to the transformation of sound-induced mechanical signals into a rate code in the SGN[10]. Indeed, the IHC ribbon synapse is highly specialized for indefatigable sound transmission at rates of hundreds of Hertz with high temporal precision, and is of critical importance for presynaptic mechanisms of sound encoding. Previous studies have revealed that ribbon synapses vary greatly in size and number at different frequency regions in the adult mouse cochlea[11,12], likely reflecting structural adaptation to the particular sound coding for survival needs. Recently, experimental animal studies have demonstrated that cochlear synaptopathy contributes to multiple forms of hearing impairments, including noise-induced hearing loss, age-related hearing loss, and hereditary hearing loss[13,14]. Thus, methods for identifying correlated changes in synaptic number, structure, and function at specific frequency regions have been increasingly employed in studies of auditory development and inner ear disease, using models generated via experimental manipulation of genetic or environmental variables[15-17].

In the current report, we present a protocol for analyzing the synaptic number, structure, and function at a specific frequency region of the basilar membrane in adult mice. Cochlear frequency localization is performed using a given place-frequency map in combination with a cochleogram. The normal morphological characteristics of cochlear ribbon synapses are evaluated via presynaptic and postsynaptic immunostaining. The functional status of cochlear ribbon synapses is determined based on the suprathreshold amplitudes of ABR wave I. With minor alterations, this protocol can be used to examine physiological or pathological conditions in other animal models, including rats, guinea pigs, and gerbils.

PROTOCOL:

All procedures were carried out in accordance with the US National Institutes of Health Guide for the Care and Use of Laboratory Animals. The study protocol was approved by the Institutional Animal Care and Use Committee of Capital Medical University, Beijing, China.

1. Animal selection

1.1. For all experiments, use adult C57BL/6J male mice (8 weeks old) as the animal model.

NOTE: C57BL/6J mice carrying a splice variant of the *Cdh23* exhibit accelerated senescence in the auditory system, reflected as a 40% loss of ribbon synapses at the basal turn of the cochlea and a 10% loss at the middle turn by 6 months of age, followed by a rapid increase of this loss in the whole cochlea with age[18,19]. Thus, we advise caution when using C57BL/6J mice older than 6 months for auditory research. Other strains of mice can be used depending on specific experimental aims.

1.2. Inspect the mice using a professional diagnostic pocket otoscope to rule out outer or middle ear pathologies prior to hearing assessments. Potential signs may include fluid or pus in the external auditory canal, redness and swelling in local tissue, and tympanic membrane perforation.

NOTE: Although this is rarely encountered, once identified, mice with outer or middle ear diseases should be excluded.

2. Hearing assessment

2.1. Anesthetize mice using an intraperitoneal injection of a mixture of ketamine hydrochloride (100 mg/kg) and xylazine hydrochloride (10 mg/kg). Judge the depth of anesthesia via painful stimuli (e.g., toe-pinch reflex).

NOTE: When the toe-pinch reflex is completely absent, the animal has reached an adequate depth of anesthesia for auditory testing. If more time is required for bilateral ABR recordings, administer a lower dosage (one-fifth the original dosage) of anesthetics to restore the original anesthetic plane. Take care to avoid anesthetic overdose, as this may lead to death in mice.

2.2. Maintain the anesthetized animal's body temperature at 37.5 °C using a thermoregulating heating pad. Place the anesthetized animal in an electrically and acoustically shielded room to avoid interference throughout the hearing test.

NOTE: Maintain the physiological temperature during the entire procedure until the animal is totally awake, in order to prevent death caused by post-anesthesia hypothermia.

2.3. Place subdermal needle electrodes (20 mm, 28 G) at the vertex of the skull (recording electrode), in the ipsilateral parotid region below the pinna of measured ear (reference electrode), and in the contralateral parotid region (ground electrode), with a depth of 3 mm under the skin of the mouse head, respectively[20].

2.4. Use a closed-field speaker to perform acoustic stimulation via a 2 cm plastic tube with a cone-shaped tip. Fit the tip into the external ear canal[21].

NOTE: Ensure that the electrical impedance in the recording and reference electrodes is less than 3 kOhm (usually 1 kOhm). If the impedance is high, change the insertion site of the electrode, clean the electrode with alcohol, or replace the electrode to avoid alterations in ABR wave amplitude.

2.5. For ABR recording, generate tone pips (3 ms duration, 1 ms rise/fall times, at a rate of 21.1/s, frequency: 4–48 kHz) and present them at decreasing SPLs from 90 to 10 dB in 5–10 dB SPL steps[20]. During this step, the responses are amplified (10,000 times), filtered (0.1–3 kHz), and averaged (1,024 samples/stimulus level).

NOTE: ABRs are collected for each stimulus level in 10 dB steps, with additional 5 dB steps near the threshold.

2.6. At each frequency, determine the ABR threshold, which refers to the minimal SPL resulting in a reliable ABR recording with one or more distinguishable waves that can be clearly identified by visual inspection (**Figure 1**).

NOTE: It is usually necessary to repeat the process for low SPLs around the threshold to ensure the consistency of the waveforms. The response threshold is the lowest stimulus level at which the waveform can be observed, when a decrease of 5 dB would lead to the disappearance of the waveform.

3. Cochlear tissue processing

3.1. After ABR recording, euthanize the anesthetized mice via cervical dislocation, decapitate them, expose the bulla from the ventral side, and open with sharp scissors to gain access to the cochlea.

3.2. Using a fine forceps, remove the temporal bones, sever the stapes artery, remove the stapes from the oval window, and rupture the round window membrane. Make a small hole at the apex of the cochlea by gently rotating the tip of a needle (13 mm, 27 G).

3.3. Fix the isolated bones with 4% (wt/vol) paraformaldehyde in 0.1 M phosphate-buffered saline (PBS, pH 7.4) overnight at 4 °C. Using a fine-tipped pipette, gently flush fixative through the perilymphatic spaces via application to the oval or round windows (as an inlet) and the opening at the apex (as an outlet).

NOTE: Some proteins require a short duration of fixation to avoid destruction of their epitopes for immunolabeling. In such cases, incubate bones in 4% paraformaldehyde at room temperature (RT) for 2 h, depending on the manufacturer's instructions for immunohistochemistry. Fixation can also be performed via cardiac perfusion to remove the cochlear blood, avoiding background noise due to non-specific staining at later stages, particularly in mouse models of cochlear synaptopathy.

3.4. Rinse the bones three times for 5 min with 0.1 M cold PBS to remove residual paraformaldehyde. Decalcify the bones with 10% ethylenediaminetetraacetic acid (EDTA) either at RT for 4 h or at 4 °C for 24 h via gentle shaking in a horizontal shaker at 20 rpm. EDTA can be refreshed midway.

NOTE: Decalcification times are subject to the concentration of EDTA and users' preferences. Decalcified tissue should maintain a certain degree of toughness, which facilitates the manipulation of isolating cochlear whole-mounts at later steps. Temporal bones can be decalcified in 10% EDTA with rotation, allowing researchers to leave the laboratory following ABR

tests and fixation experiments. The decalcification time is flexible within the range of 20 to 30 h at 4 °C.

3.5. Transfer one decalcified temporal bone from EDTA to 0.1 M PBS. Use #3, #5 Dumont forceps and the 27 G needle to dissect the apical, middle and basal cochlear regions in turn and then dissect the cochlea out of the bone under a stereo dissection microscope (as previously described[22]). Make a series of small cuts along the spiral ligament using a razor blade, and remove the tectorial membrane and Reissner's membrane (**Figure 2**).

NOTE: As long as the dissected cochlea is intact, this process can be modified according to the individual operator's usual protocol.

3.6. Further dissect the remaining auditory epithelium including the spiral limbus into individual cochlear turns (apex, middle, and base with hook region) for whole-mount preparations.

3.7. Under a 40x oil objective of a light microscope, measure the basilar membrane length with a 250 µm scale placed in the eyepiece, which can be adjusted along the stereocilia of the IHCs.

3.8. Calculate the length of each cochlear turn by adding all segment lengths (250 µm per segment), and concomitantly obtain the total length of the basilar membrane by summing the lengths of each turn.

3.9. Convert the total length of the basilar membrane including the hook region into a percentage based on distance from the cochlear apex (0% refers to the cochlear apex, 100% to the cochlear base).

3.10. Convert this distance into the cochlear characteristic frequency using a logarithmic function ($d(\%) = 1 - 156.5 + 82.5 \times \log(f)$, with a slope of 1.25 mm/octave of frequency, where d is the normalized distance from the cochlear apex in percent, f is the frequency in kHz), as previously described[5,6]. Thus frequency range in a corresponding area of the basilar membrane on each cochlear turn can be acquired.

4. Immunofluorescence staining

4.1. After dissection, place each cochlear turn in a separate 2.5 mL centrifuge tube and incubate cochlear turns in 10% goat serum/PBS/0.1% Triton X-100 for 1 h at RT on a rotator.

4.2. Remove the above blocking/permeabilization solution from each tube using a 200 µL pipette tip under a dissection microscope and incubate the specimens with primary antibodies diluted in 5% goat serum/PBS/0.1% Triton X-100 overnight at 4 °C on a rotator.

NOTE: For immunolabeling of cochlear synaptic ribbons, use the presynaptic marker mouse anti-carboxyl-terminal binding protein 2 IgG1 (CtBP2, labeling the B domain of the RIBEYE scaffolding

protein, 1:400) and the postsynaptic marker mouse anti-glutamate receptor 2 IgG2a (GluR2, labeling a subunit of the AMPA receptor, 1:200)[23].

4.3. Rinse three times for 5 min with 0.1 M cold PBS to remove residual primary antibodies and incubate the specimens with secondary antibodies diluted in 5% goat serum/PBS/0.1% Triton X-100 at RT for 2–3 h in darkness on a rotator.

NOTE: Prepare appropriate secondary antibody mixtures using goat anti-mouse Alexa Fluor 568 (IgG1, 1:500) and goat anti-mouse Alexa Fluor 488 (IgG2a, 1:500), which are complementary to the primary antibodies used in step 4.2. To improve labeling efficiency for synaptic ribbons, we recommend selecting specific secondary antibodies. Some labs extend incubation with secondary antibodies to increase GluR2 immunolabeling[24].

4.4. Rinse three times for 5 min with 0.1 M PBS to remove residual secondary antibodies and transfer the specimens from 2.5 mL centrifuge tubes to 35 mm plates containing 0.1 M PBS.

4.5. Place a drop of mounting medium containing 4',6-diamidino-2-phenylindole (DAPI) onto the slide and transfer the specimens from PBS to the mounting medium. Place one edge of a coverslip on the slide and release to let the coverslip fall gently.

NOTE: To ensure that the hair cells face upward and that no folding or twisting of cochlear specimens occurs during the procedure, mount cochlear specimens under a stereo dissection microscope.

4.6. Place the slides in a slide box at 4 °C overnight to let slides dry and then image under a laser confocal microscope.

5. Morphological evaluation of cochlear ribbon synapses

5.1. Image slides using a confocal microscope with three lasers—a 405 nm UV diode, a 488 nm argon laser, and a 561 nm diode-pumped solid-state (DPSS) laser to excite DAPI (Excitation spectrum 409–464 nm), Alexa Fluor 488 (Excitation spectrum 496–549 nm) and Alexa Fluor 568 (Excitation spectrum 573–631 nm), respectively.

5.2. Acquire confocal z-stacks over a distance of 8 µm from each cochlear turn using a 63x high-resolution oil immersion lens.

NOTE: Once defined, all parameters for digitizing photomicrographs should be saved and applied uniformly to all slides.

5.3. For synaptic punctum counts, set the z-stacks (0.3 µm step size) to span the entire length of IHCs, thereby ensuring that all synaptic puncta can be imaged.

5.4. Merge the images containing puncta in a z-stack to obtain the z-axis projection, and import to the image-processing software.

5.5. Divide synaptic total counts in each z-stack at specific frequency regions by the number of IHCs (equal to the DAPI nuclear manual counts) to calculate the number of synaptic puncta for each IHC. At each specific frequency region, average all synaptic puncta in three images of different microscopic fields containing 9–11 IHCs.

5.5.1. Outline the region of interests (ROIs) including the basolateral regions of each IHC using freehand selections button. Use the **measure** function for automatic quantification of puncta, and the **watershed** function to distinguish between closely adjacent spots.

5.5.2. After each automated counting, perform visual inspections with manual corrections to ensure puncta counting reliable.

NOTE: Experimenters should remain blinded as to whether the slide is from the apex, middle, or basal turn of the cochlea.

5.6. Visually assess synaptic structure and distribution, to manually isolate individual IHCs from their neighbors by the **Brush Tool** to better visualize the cytoskeletal architecture and synaptic localization.

5.7. To inspect the juxtaposition of presynaptic ribbons (CtBP2) and postsynaptic receptor patches (GluR2), extract the voxel space around ribbon by the **Rectangular Marquee Tool** and isolate individual ribbon by **Image Cutting**. Through clicking **Image > Image Size**, acquire a thumbnail array of these miniature projections, which can then be used to identify paired synapses (appeared as closely juxtaposed pairs of CtBP2-positive and GluR2-positive puncta) versus orphan ribbons (lacking postsynaptic glutamate receptor patches) (**Figure 3**).

NOTE: Normal cochlear synapses appear as combined immunolabeling of the presynaptic ribbon within the hair cell (anti-CtBP2) and the postsynaptic glutamate receptor patch on the auditory nerve terminal (anti-GluR2)[25]. Some labs use confocal projections in conjunction with 3D modeling to quantify synaptic patch size or volume[26,27]. Prior to significant loss of ribbon synapses, ribbons exhibiting changes in size or without paired glutamate receptor patches are likely indicative of synaptic dysfunction[27,28].

6. Functional evaluation of cochlear ribbon synapses

6.5. Collect all ABR waves for each frequency stimulus presented at an SPL of 90 dB for the analysis of suprathreshold ABR wave I amplitudes.

NOTE: Neurophysiological and morphological studies have demonstrated that low spontaneous-rate, high-threshold fibers are especially vulnerable to aging and noise exposure[29,30]. Although the simple loss of ribbon synapses cannot affect ABR thresholds, it commonly results in significant

reductions in ABR wave I amplitudes, because these afferents including low spontaneous-rate, high-threshold fibers and high spontaneous-rate, low-threshold fibers contribute heavily to the summed activities of cochlear nerve fibers[28,29,31]. A suprathreshold intensity of 90 dB SPL is selected here.

6.6. Determine peak-to-peak wave I amplitude using an offline analysis program (**Figure 4**). Each wave I in the ABR test consists of a starting positive (p) deflection and the subsequent negative (n) deflection. ABR wave I amplitude is defined as the difference in voltage between Ip (the positive peak of wave I) and In (the negative peak of wave I)[29].

NOTE: In pathological conditions, cochlear synaptopathy can be determined based on the suprathreshold amplitudes of ABR wave I, which reflect the summed onset responses of SGNs evoked by sound. However, cochlear sensitivity that is not compromised due to OHC dysfunction is a prerequisite for this method.

REPRESENTATIVE RESULTS:

ABR hearing tests were performed for 10 C57BL/6J mice (8 weeks of age) under anesthesia. ABRs were elicited using tone burst stimuli at 4, 8, 16, 32, and 48 kHz. The hearing threshold of each animal was visually detected by distinguishing at least one clear waveform in the ABR. All mice exhibited ABR thresholds in response to tone bursts, ranging between 25 and 70 dB SPL depending on the frequency of the stimulus. Our results indicated that the hearing threshold was lowest at 16 kHz (**Figure 1**), corresponding to approximately 43% distance from the cochlear apex (**Figure 2**), suggesting that acoustic sensitivity is significantly reduced in other cochlear regions.

Cochlear whole-mounts were isolated from temporal bones in adult mice under a stereo dissection microscope (**Figure 2A**). Whole-mounts of the auditory epithelium were dissected into three pieces, the lengths of which were measured and eventually converted into percent distance from the cochlear apex. The frequency location on the basilar membrane of each cochlear turn was calculated using a logarithmic function, as previously described[5,6] (**Figure 2B**).

To evaluate the morphological characteristics of cochlear ribbon synapses, antibodies against CtBP2 and GluR2 were used to label presynaptic and postsynaptic structures, respectively. In normal ears of adult mice, immunostaining revealed juxtaposed pairs of synaptic ribbons and glutamate receptor patches studding the surface of the basolateral membrane of IHCs, with 8–20 pairs per IHC (**Figure 3A**). Although the vast majority of puncta appeared as juxtaposed pairs in normal ears, orphan ribbons could be observed rarely at high magnification (**Figure 3B**). Counts of IHC ribbon synapses (immunopositive spots for both CtBP2 and GluR2) were highest at the 16 kHz region, significantly decreasing as the distance from this location increased (**Figure 3C**). The synaptic counts determined based on confocal projections provide an estimate of the maximum number of auditory nerve fibers that transmit information from the cochlea to the brain[29].

The functional status of cochlear ribbon synapses was investigated in all adult mice based on ABR wave I amplitudes, which provide information regarding the functional integrity of auditory nerve fibers[29,31]. ABR wave I amplitudes at each frequency of the stimulus presented at a sound

pressure level of 90 dB were measured from peak to the following trough, as shown in **Figure 4A**. ABR wave I amplitude was highest at a frequency of 16 kHz, corresponding to the lowest hearing threshold, and amplitude values significantly decreased as distance from this location increased (**Figure 4B**). This result is consistent with the observed alterations in ribbon synapse counts, indicating that synapses within this cochlear region may exhibit the most vivid synaptic function. Furthermore, in previous mouse studies of noise-induced and age-related cochlear neurodegeneration, suprathreshold amplitudes of ABR wave I decreased in proportion to ribbon loss, indicating that ABR wave I amplitude is highly correlated with the degree of cochlear synaptopathy[29,31].

FIGURE AND TABLE LEGENDS:

Figure 1: Hearing Assessment. ABR threshold comparisons among different frequencies of tone burst stimuli demonstrated that the hearing threshold was lowest at 16 kHz in 10 adult C57BL/6J mice. The ABR response was significantly elevated at other frequency regions (one-way ANOVA with Dunnett's multiple comparison *post hoc* test; *: $P < 0.01$, n = 20 ears). Data are expressed as the mean ± SEM.

Figure 2: Cochlear frequency localization in mice. (A) A representative image of the full explanted cochlea, which has been dissected out of the temporal bone under a stereo dissection microscope. **(B)** The mouse cochlea is divided into apical, middle, and basal turns, where the cochlear lateral wall is removed. Red circles on the fragments of the cochlear basilar membrane indicate the frequency locations and their corresponding normalized positions in the cochlea (0% refers to the cochlear apex, 100% to the cochlear base). Scale bar = 250 µm.

Figure 3: Confocal analysis of cochlear ribbon synapses in mice. (A) Representative images of ribbon synapses for the 4, 8, 16, 32, and 48 kHz regions, immunostained for presynaptic ribbons (CtBP2, red) and postsynaptic structures (GluR2, green). White dashed lines are used to outline inner hair cells for reference. Scale bar = 10 µm. **(B)** High-power thumbnails from confocal z-stacks show that these ribbon synapses appeared as closely juxtaposed pairs of CtBP2-positive (red) and GluR2-positive (green) puncta (left and middle), whereas orphan ribbons (right) lacking postsynaptic glutamate receptor patches were very rare. Scale bar = 0.5 µm. **(C)** Quantitative analysis of paired ribbon puncta with all presynaptic and postsynaptic elements revealed that the number of synaptic puncta per inner hair cell was significantly higher at the 16 kHz region than in other frequency regions (one-way ANOVA with Dunnett's multiple comparison *post hoc* test; *: $P < 0.01$, n=6 ears). Data are expressed as the mean ± SEM.

Figure 4: Analysis of ABR wave I amplitudes in mice. (A) Representative ABR waveform from an 8 weeks old C57BL/6J mouse exposed to a 16 kHz pure tone stimulus at an intensity of 90 dB (stimulus onset at 0 ms). Roman numerals mark the peaks of the ABR waves. Dotted lines mark the wave I peak and trough, indicating the amplitude. **(B)** Quantitative analysis of average wave I amplitudes in response to the 4, 8, 16, 32, and 48 kHz stimuli presented at a sound pressure level of 90 dB. ABR wave I amplitudes were highest at the frequency of 16 kHz and significantly

lower at other frequencies (one-way ANOVA with Dunnett's multiple comparison *post hoc* test; *: $P < 0.01$, n = 20 ears). Data are expressed as the mean ± SEM.

DISCUSSION:

Since cochlear synaptopathy was first characterized in adult mice with a temporary threshold shift (TTS) induced by 8–16 kHz octave band noise at 100 dB SPL for 2 h[31], researchers have increasingly investigated the effects of synaptopathy in various mammals, including monkeys and humans[32,33]. In addition to noise exposure, several other conditions have been associated with cochlear synaptopathy (e.g., aging, the use of ototoxic drugs, and genetic mutations), leading to short-term disruption of suprathreshold audition, followed by irreversible degeneration of the auditory nerve. In the early phase of cochlear insult, synaptopathy often occurs at a specific frequency location, especially in experimental models in which damage to IHC synapses is restricted to select frequency regions[24,31]. Therefore, our protocol is significant in that it enables the investigation of synaptic morphology and function at a specific frequency region.

The cochlear place-frequency map can be used to discriminate normal and abnormal auditory function, further reflecting normal and abnormal area in the inner ear. Since surface preparation techniques were first used to plot intact and missing hair cells in the different cochlear turns, the cochleogram has become a routine method for quantifying hair cell loss[6]. Therefore, to correlate morphological insults in the cochlea to relevant physiological changes, it is reasonable to include a place-frequency map on the cochleogram. This method allows one to determine the number and structure of synapses based on their positions along the cochlear basilar membrane in relation to established cochlear place-frequency maps, thereby providing sufficient information for detailed comparisons between histological and physiological outcomes. However, some studies assess synaptopathy based on cochlear segment or distance along the cochlear duct, which does not allow for direct comparisons among individual cochleae due to intra-species variations in basilar membrane length. Thus, it is particularly important to standardize the cochleogram by converting individual cochlear lengths from millimeters to a relative percentage.

Synaptopathy can be confirmed via visualization of immunostaining for CtBP2 protein (the synaptic isoform "ribeye") in the basolateral regions of IHCs. These CtBP2-positive patches can serve as a structural marker for quantification of presynaptic ribbons, and the presence of fewer patches usually indicates presynaptic loss. Although previous studies have reported that 98% of presynaptic ribbons are paired with post-synaptic terminals in the normal ear[30], the simple number of CtBP2-positive patches may not be accurate for quantitative analysis of complete synapses, as this may lead to overestimation of synapse counts in the injured ear by involving "orphans" (presynaptic ribbons unpaired with postsynaptic terminals). To improve the accuracy of estimating synapse number, additional antibodies against postsynaptic structure such as GluA2, GluA2/3, or PSD-95 are used. The postsynaptic density protein PSD-95, a membrane-associated guanylate kinase (MAGUK) scaffolding protein, can be labeled using an antibody against PSD-95, which is mostly observed at the contacts between hair cells and SGN fiber endings[34,35]. However, the antibody against GluR2 is more specific for AMPA-type ionotropic glutamate receptors in the postsynaptic membrane, which can more reliably identify ribbon synapses (juxtaposed pairs of immunofluorescent puncta of presynaptic CtBP2 and postsynaptic

GluR2)[15]. In addition to morphological analysis, histological analysis of complete synapses can be used as a functional indicator for synaptopathy. In adult mice with cochlear synaptopathy, reductions in ABR wave I amplitude following the presentation of moderate- to high-level tone stimuli occur at frequencies tonotopically related to regions of synaptic loss[26,29]. Synapse counts obtained using this method are limited in that it takes approximately 10 minutes to scan one site on the basilar membrane. Furthermore, to evaluate spatial variations in synaptic number and morphology based on IHC location, it is necessary to accurately identify the boundary of the ICH body (e.g., via myosin VIIa staining) and to perform particular image-processing steps[26]. Using such methods, previous studies have confirmed that synaptic loss is greater on the modiolar side of the IHC than on the pillar side in animal models of noise-induced degeneration[26].

Previous studies have demonstrated that low spontaneous-rate, high-threshold fibers are more susceptible to noise damage than high spontaneous-rate, low-threshold fibers in animal models of restricted synaptopathy[26,30]. These studies provide the rationale for using suprathreshold amplitudes of ABR wave I (measured using moderate- to high-level tone stimuli) to assess synaptic function in animal models with normal ABR threshold and distortion product otoacoustic emissions (DPOAEs). Because wave I of the ABR reflects the summed neural responses of auditory nerve fibers, when synaptopathy is assessed via ABR wave I amplitude, DPOAE testing should also be performed to exclude OHC damage, which also can reduce ABR amplitudes due to the disruption of mechanoelectric transduction. Although the first wave of the compound action potential (CAP), which is measured from round-window electrodes, also represents summed activity of the cochlear nerve, this method is more invasive and complex than ABR measurements. If DPOAE responses return to normal after temporary threshold shifts in noise-exposed mice[31] or they have not yet deteriorated in aging mice[29], the suprathreshold amplitude of ABR wave I can strongly predict the degree of cochlear synaptopathy, since affected neurons are silenced when their synaptic connections to IHCs are disrupted. However, if cochlear sensitivity is reduced due to various factors (e.g., OHC dysfunction), decreases in ABR wave I amplitude can no longer be attributed solely to synaptic loss because they will reflect the combination of all cochlear damage. Therefore, controlled experimental conditions for synaptopathy-restricted model preparation are required to ensure that cochlear sensitivity is not compromised by other factors. Unfortunately, although ABR wave I amplitude provides an objective measure of auditory nerve fiber loss in animals, it is difficult to measure in humans. Moreover, mixed pathologies involving synaptopathy, loss of hair cells, and the presence of other abnormalities in the cochlea may co-occur in humans, limiting the use of ABR wave I amplitude measurements in clinical settings. ABR wave latency is calculated as the time in milliseconds from the onset of the stimulus to the positive peak of each wave, providing insight into the transmission times along the auditory pathway. No significant changes in wave I latency have been observed in mouse models of noise-induced or age-related cochlear synaptopathy[36]. However, some evidence suggests that the effects of masking noise on ABR wave V latency can be used to diagnose cochlear synaptopathy in humans[37].

Several recent studies have supported the notion that cochlear synaptopathy is the primary initial event associated with hidden hearing loss, tinnitus, and hyperacusis. Although the concept of cochlear synaptopathy in inner ear diseases has now been firmly established, its detailed impact

on hearing ability remains unknown. The protocol presented in the current study enables the investigation of morphology and function in cochlear ribbon synapses within a specific frequency region. Thus, this protocol can be used to investigate cochlear synaptopathy, its underlying mechanisms, and the efficacy of potential therapeutic interventions in various experimental animal models.

ACKNOWLEDGMENTS:

This work was supported by the National Natural Science Foundation of China (81770997, 81771016, 81830030); the joint funding project of Beijing Natural Science Foundation and Beijing Education Committee (KZ201810025040); the Beijing Natural Science Foundation (7174291); and the China Postdoctoral Science Foundation (2016M601067).

DISCLOSURES:

The authors have no conflicts of interest to disclose.

REFERENCES:

1. Lie, A., Skogstad, M., Johnsen, T. S., Engdahl, B., Tambs, K., The prevalence of notched audiograms in a cross-sectional study of 12,055 railway workers. *Ear and Hearing* . **36** (3), e86-92 (2015).

2. Fettiplace, R., Hair cell transduction, tuning, and synaptic transmission in the mammalian cochlea. *Comprehensive Physiology.* **7** (4), 1197-1227 (2017).

3. Liberman, M. C., The cochlear frequency map for the cat: labeling auditory-nerve fibers of known characteristic frequency. *Journal of the Acoustical Society of America.* **72** (5), 1441-9 (1982).

4. Fettiplace, R., Kim, K. X., The physiology of mechanoelectrical transduction channels in hearing. *Physiological Reviews.* **94** (3), 951-86 (2014).

5. Muller, M., von Hunerbein, K., Hoidis, S., Smolders, J. W., A physiological place-frequency map of the cochlea in the CBA/J mouse. *Hearing Research.* **202** (1-2), 63-73 (2005).

6. Viberg, A., Canlon, B., The guide to plotting a cochleogram. *Hearing Research.* **197** (1-2), 1-10 (2004).

7. Paquette, S. T., Gilels, F., White, P. M., Noise exposure modulates cochlear inner hair cell ribbon volumes, correlating with changes in auditory measures in the FVB/nJ mouse. *Scientific Reports.* 6, 25056 (2016).

8. Fernandez, K. A., Jeffers, P. W., Lall, K., Liberman, M. C., Kujawa, S. G., Aging after noise exposure: acceleration of cochlear synaptopathy in "recovered" ears. *Journal of Neuroscience.* **35** (19), 7509-20 (2015).

9. Wichmann, C., Moser, T., Relating structure and function of inner hair cell ribbon synapses. *Cell and Tissue Research.* **361** (1), 95-114 (2015).

10. Matthews, G., Fuchs, P., The diverse roles of ribbon synapses in sensory neurotransmission. *Nature Reviews Neuroscience.* **11** (12), 812-22 (2010).

11. Liberman, L. D., Liberman, M. C., Postnatal maturation of auditory-nerve heterogeneity, as seen in spatial gradients of synapse morphology in the inner hair cell area. *Hearing Research.* **339**, 12-22 (2016).

12. Yang, L. et al. Maximal number of pre-synaptic ribbons are formed in cochlear region corresponding to middle frequency in mice. *Acta Oto-Laryngologica.* **138** (1), 25-30 (2018).
13. Liberman, M. C., Kujawa, S. G., Cochlear synaptopathy in acquired sensorineural hearing loss: Manifestations and mechanisms. *Hearing Research.* **349**, 138-147 (2017).
14. Moser, T., Starr, A., Auditory neuropathy--neural and synaptic mechanisms. *Nature Reviews Neurology*. **12** (3), 135-49 (2016).
15. Yu, W. M. et al. A Gata3-Mafb transcriptional network directs post-synaptic differentiation in synapses specialized for hearing. *Elife.* 2, e01341 (2013).
16. Buniello, A. et al. Wbp2 is required for normal glutamatergic synapses in the cochlea and is crucial for hearing. *EMBO Molecular Medicine.* **8** (3), 191-207 (2016).
17. Gilels, F., Paquette, S. T., Beaulac, H. J., Bullen, A., White, P. M., Severe hearing loss and outer hair cell death in homozygous Foxo3 knockout mice after moderate noise exposure. *Scientific Reports.* **7** (1), 1054 (2017).
18. Kane, K. L. et al. Genetic background effects on age-related hearing loss associated with Cdh23 variants in mice. *Hearing Research.* **283** (1-2), 80-8 (2012).
19. Jiang, X. W., Li, X. R., Zhang, Y. P., Changes of ribbon synapses number of cochlear hair cells in C57BL/6J mice with age (Delta). *International Journal of Clinical and Experimental Medicine*. **8** (10), 19058-64 (2015).
20. Akil, O., Oursler, A., Fan, K., & Lustig, L., Mouse auditory brainstem response testing. *BIO-Protocol*. **6** (6), (2016).
21. Zhou, X., Jen, P. H.-S., Seburn, K. L., Frankel, W. N., Zheng, Q. Y., Auditory brainstem responses in 10 inbred strains of mice. *Brain Research*. **1091** (1), 16-26, (2006).
22. Montgomery, S. C., Cox, B. C., Whole mount dissection and immunofluorescence of the adult mouse cochlea. *Journal of Visualized Experiments.* (107) (2016).
23. Schmitz, F., Konigstorfer, A., Sudhof, T. C., RIBEYE, a component of synaptic ribbons: a protein's journey through evolution provides insight into synaptic ribbon function. *Neuron.* **28** (3), 857-72 (2000).
24. Suzuki, J., Corfas, G., Liberman, M. C., Round-window delivery of neurotrophin 3 regenerates cochlear synapses after acoustic overexposure. *Scientific Reports.* **6**, 24907 (2016).
25. Rutherford, M. A., Resolving the structure of inner ear ribbon synapses with STED microscopy. *Synapse.* **69** (5), 242-55 (2015).
26. Liberman, L. D., Liberman, M. C., Dynamics of cochlear synaptopathy after acoustic overexposure. *Journal of the Association for Research in Otolaryngology.* **16** (2), 205-19 (2015).
27. Gilels, F., Paquette, S. T., Zhang, J., Rahman, I., White, P. M., Mutation of Foxo3 causes adult onset auditory neuropathy and alters cochlear synapse architecture in mice. *Journal of Neuroscience.* **33** (47), 18409-24 (2013).
28. Wan, G., Gomez-Casati, M. E., Gigliello, A. R., Liberman, M. C., Corfas, G., Neurotrophin-3 regulates ribbon synapse density in the cochlea and induces synapse regeneration after acoustic trauma. *Elife.* **3** (2014).
29. Sergeyenko, Y., Lall, K., Liberman, M. C., Kujawa, S. G., Age-related cochlear synaptopathy: an early-onset contributor to auditory functional decline. *Journal of Neuroscience.* **33** (34), 13686-94 (2013).
30. Furman, A. C., Kujawa, S. G., Liberman, M. C., Noise-induced cochlear neuropathy is selective for fibers with low spontaneous rates. *Journal of Neurophysiology.* **110** (3), 577-86 (2013).

31. Kujawa, S. G., Liberman, M. C., Adding insult to injury: cochlear nerve degeneration after "temporary" noise-induced hearing loss. *Journal of Neuroscience.* **29** (45), 14077-85 (2009).
32. Valero, M. D. et al. Noise-induced cochlear synaptopathy in rhesus monkeys (Macaca mulatta). *Hearing Research.* **353**, 213-223 (2017).
33. Viana, L. M. et al. Cochlear neuropathy in human presbycusis: Confocal analysis of hidden hearing loss in post-mortem tissue. *Hearing Research.* **327**, 78-88 (2015).
34. Tong, M., Brugeaud, A., Edge, A. S., Regenerated synapses between postnatal hair cells and auditory neurons. J*ournal of the Association for Research in Otolaryngology.* **14** (3), 321-9 (2013).
35. Landegger, L. D., Dilwali, S., Stankovic, K. M., Neonatal murine cochlear explant technique as an in vitro screening tool in hearing research. *Journal of Visualized Experiments.* (124) (2017).
36. Takeda, S., Mannström, P., Dash-Wagh, S., Yoshida, T., Ulfendahl, M., Effects of Aging and Noise Exposure on Auditory Brainstem Responses and Number of Presynaptic Ribbons in Inner Hair Cells of C57BL/6J Mice. *Neurophysiology.* **49** (5), 316-26 (2017).
37. Mehraei, G. et al. Auditory brainstem response latency in noise as a marker of cochlear synaptopathy. *Journal of Neuroscience.* **36** (13), 3755-64 (2016).

Figure1

Click here to access/download;Figure;FIGURE1.tif

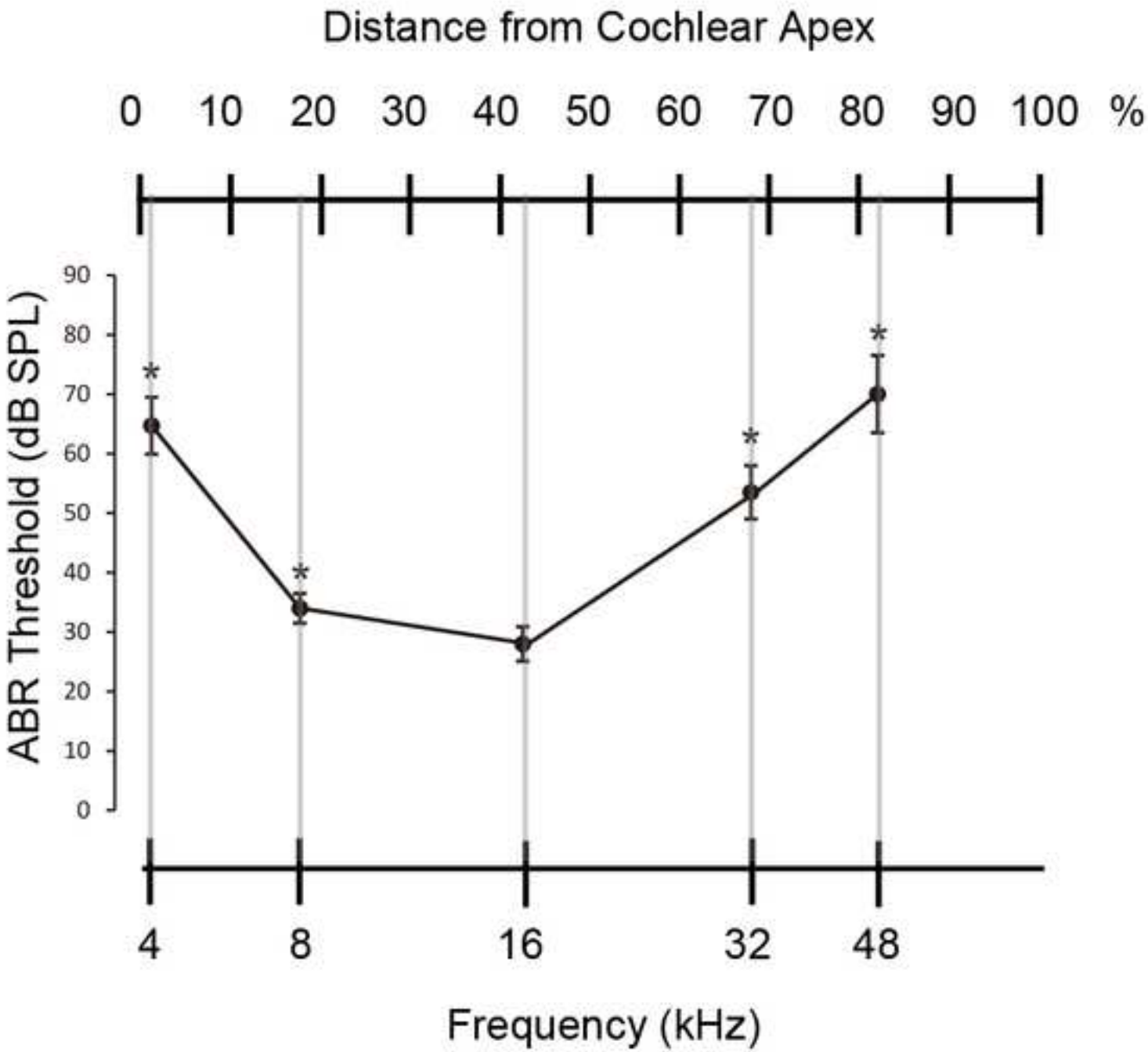

Figure2

Click here to access/download;Figure;FIGURE2.tif

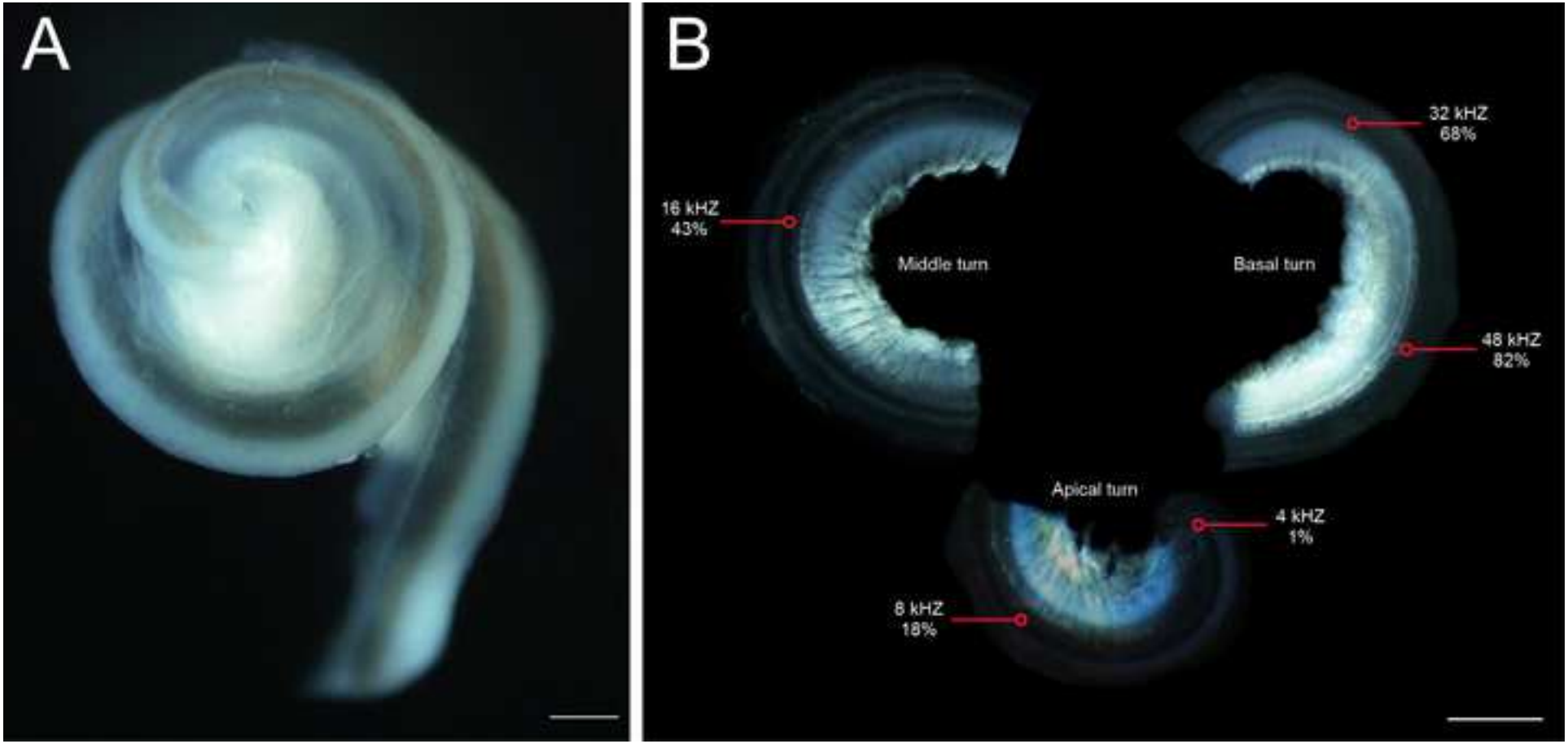

Figure3

Click here to access/download;Figure;FIGURE3.tif

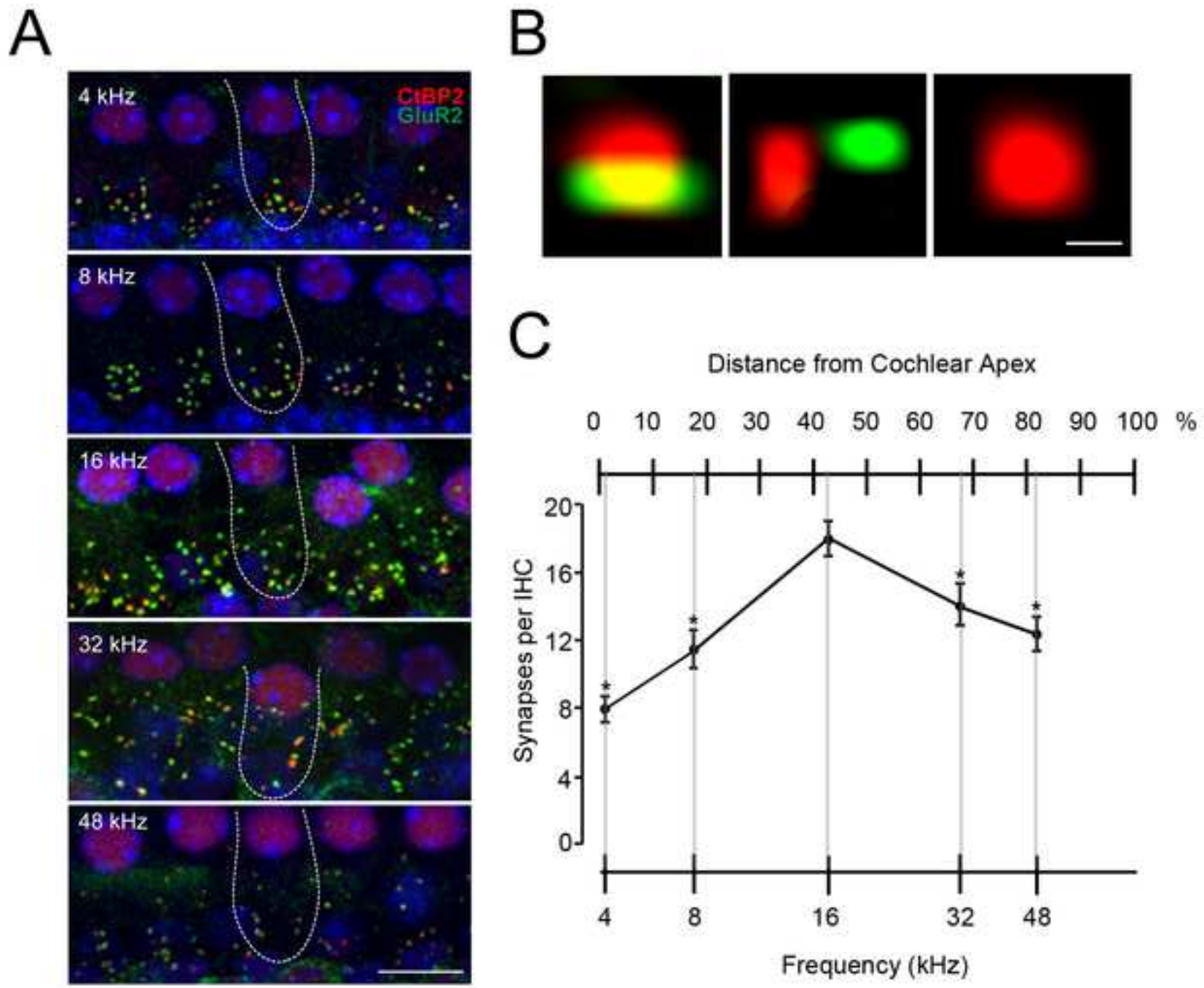

A

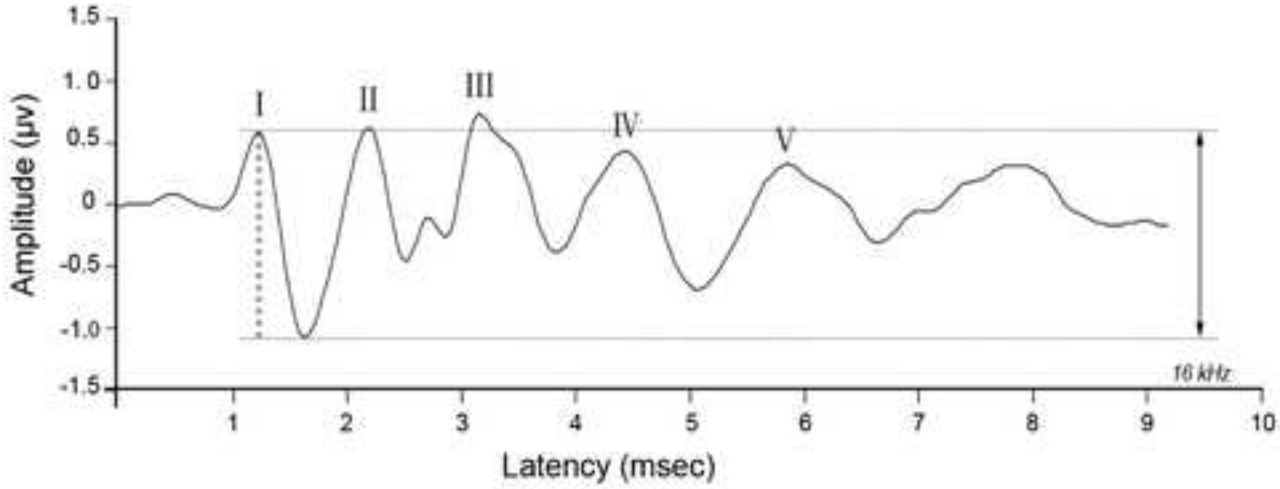

B

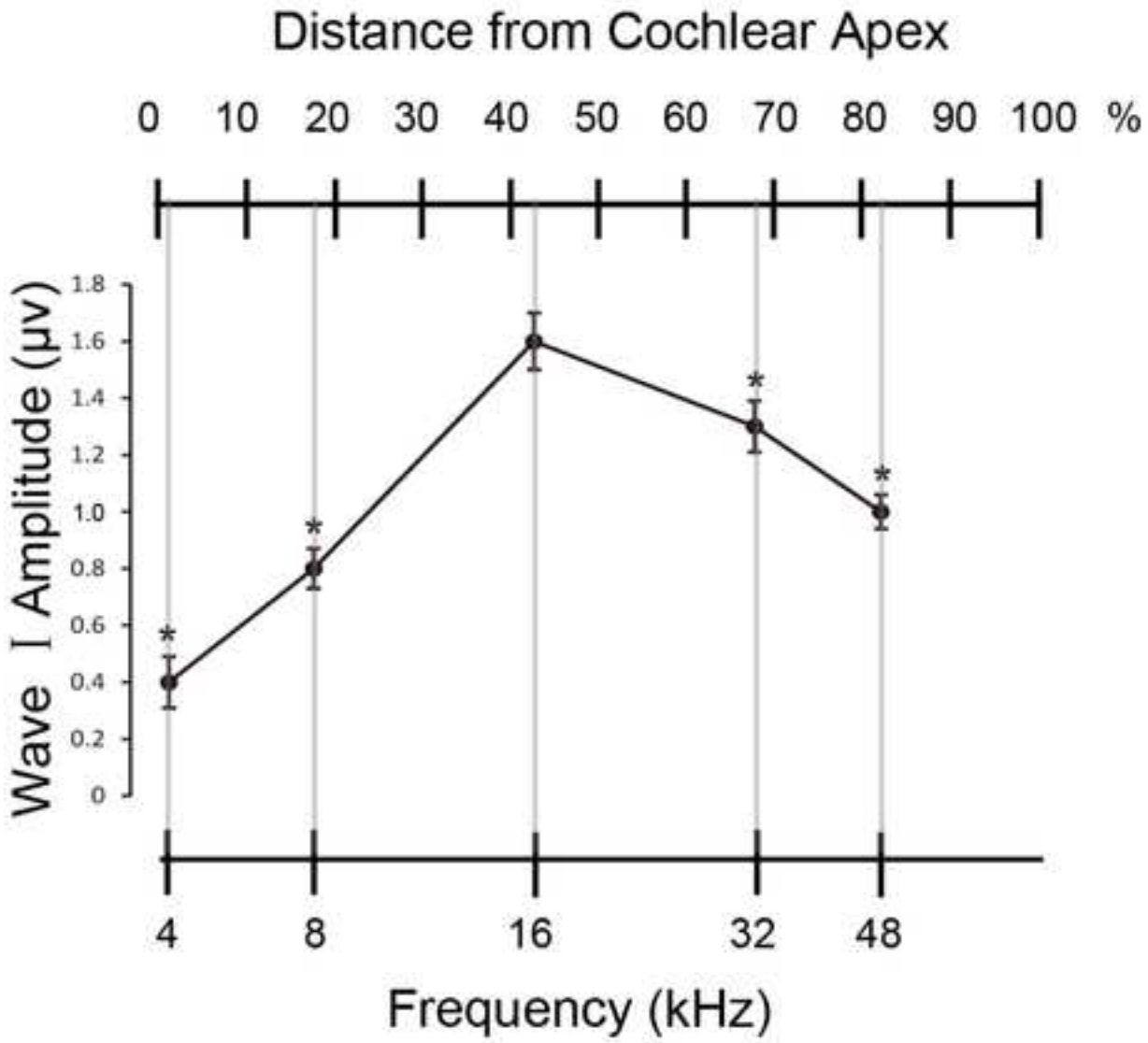

Name of Material/ Equipment	Company	Catalog Number	Comments/Description
Ketamine hydrochloride	Gutian Pharmaceutical Co., Ltd., Fujian, China	H35020148	100mg/kg
Xylazine hydrochloride	Sigma-Aldrich, St. Louis, MO, USA	X-1251	10mg/kg
TDT physiology apparatus	Tucker-Davis Technologies, Alachua, FL, USA	Auditory Physiology System III	
SigGen/BioSig software	Tucker-Davis Technologies, Alachua, FL, USA	Auditory Physiology System III	
Electric Pad	Pet Fun	11072931136	
Dumont forceps 3#	Fine Science Tools, North Vancouver, B.C., Canac	0203-3-PO	
Dumont forceps 5#	Fine Science Tools, North Vancouver, B.C., Canac	0209-5-PO	
Stereo dissection microscope	Nikon Corp., Tokyo, Japan	SMZ1270	
Goat serum	ZSGB-BIO, Beijing,China	ZLI-9021	
Anti-glutamate receptor 2, extracell	Millipore Corp., Billerica, MA, USA	MAB397	mouse
Purified Mouse Anti-CtBP2	BD Biosciences, Billerica, MA, USA	612044	mouse
Alexa Fluor 568 goat anti-mouse Ig	Thermo Fisher Scientific Inc., Waltham, MA, USA	A21124	goat
Alexa Fluor 488 goat anti-mouse Ig	Thermo Fisher Scientific Inc., Waltham, MA, USA	A21131	goat
Mounting medium containing DAP	ZSGB-BIO, Beijing,China	ZLI-9557	
Confocal fluorescent microscopy	Leica Microsystems, Wetzlar, Germany	TCS SP8 II	
Image Pro Plus software	Media Cybernetics, Bethesda, MD, USA	version 6.0	
Professional diagnostic pocket otos	Lude Medical Apparatus and Instruments Trade C	HS-OT10	
Needle electrode	Friendship Medical Electronics Co., Ltd., Xi'an,Ch	1029	20 mm, 28 G
Closed-field speaker	Tucker-Davis Technologies, Alachua, FL, USA	CF1	

jove JOURNAL OF VISUALIZED EXPERIMENTS
1 Alewife Center #200
Cambridge, MA 02140
tel. 617.945.9051
www.jove.com

ARTICLE AND VIDEO LICENSE AGREEMENT

Title of Article: Morphological and functional Evaluation of Ribbon Synapse at Specific frequency Region of the Mouse Cochlea

Author(s): Shukui Yu, Zhengde Du, Qingling Song, Tongfei Qu, Yue Qi, Wei Xiong, Lu He, Wei Wei, Ke Liu, Shusheng Gong.

Item 1: The Author elects to have the Materials be made available (as described at http://www.jove.com/publish) via:

☑ Standard Access ☐ Open Access

Item 2: Please select one of the following items:

☑ The Author is **NOT** a United States government employee.

☐ The Author is a United States government employee and the Materials were prepared in the course of his or her duties as a United States government employee.

☐ The Author is a United States government employee but the Materials were NOT prepared in the course of his or her duties as a United States government employee.

ARTICLE AND VIDEO LICENSE AGREEMENT

1. **Defined Terms.** As used in this Article and Video License Agreement, the following terms shall have the following meanings: "**Agreement**" means this Article and Video License Agreement; "**Article**" means the article specified on the last page of this Agreement, including any associated materials such as texts, figures, tables, artwork, abstracts, or summaries contained therein; "**Author**" means the author who is a signatory to this Agreement; "**Collective Work**" means a work, such as a periodical issue, anthology or encyclopedia, in which the Materials in their entirety in unmodified form, along with a number of other contributions, constituting separate and independent works in themselves, are assembled into a collective whole; "**CRC License**" means the Creative Commons Attribution-Non Commercial-No Derivs 3.0 Unported Agreement, the terms and conditions of which can be found at: http://creativecommons.org/licenses/by-nc-nd/3.0/legalcode; "**Derivative Work**" means a work based upon the Materials or upon the Materials and other pre-existing works, such as a translation, musical arrangement, dramatization, fictionalization, motion picture version, sound recording, art reproduction, abridgment, condensation, or any other form in which the Materials may be recast, transformed, or adapted; "**Institution**" means the institution, listed on the last page of this Agreement, by which the Author was employed at the time of the creation of the Materials; "**JoVE**" means MyJove Corporation, a Massachusetts corporation and the publisher of The Journal of Visualized Experiments; "**Materials**" means the Article and / or the Video; "**Parties**" means the Author and JoVE; "**Video**" means any video(s) made by the Author, alone or in conjunction with any other parties, or by JoVE or its affiliates or agents, individually or in collaboration with the Author or any other parties, incorporating all or any portion of the Article, and in which the Author may or may not appear.

2. **Background.** The Author, who is the author of the Article, in order to ensure the dissemination and protection of the Article, desires to have the JoVE publish the Article and create and transmit videos based on the Article. In furtherance of such goals, the Parties desire to memorialize in this Agreement the respective rights of each Party in and to the Article and the Video.

3. **Grant of Rights in Article.** In consideration of JoVE agreeing to publish the Article, the Author hereby grants to JoVE, subject to **Sections 4** and **7** below, the exclusive, royalty-free, perpetual (for the full term of copyright in the Article, including any extensions thereto) license (a) to publish, reproduce, distribute, display and store the Article in all forms, formats and media whether now known or hereafter developed (including without limitation in print, digital and electronic form) throughout the world, (b) to translate the Article into other languages, create adaptations, summaries or extracts of the Article or other Derivative Works (including, without limitation, the Video) or Collective Works based on all or any portion of the Article and exercise all of the rights set forth in (a) above in such translations, adaptations, summaries, extracts, Derivative Works or Collective Works and(c) to license others to do any or all of the above. The foregoing rights may be exercised in all media and formats, whether now known or hereafter devised, and include the right to make such modifications as are technically necessary to exercise the rights in other media and formats. If the "Open Access" box has been checked in **Item 1** above, JoVE and the Author hereby grant to the public all such rights in the Article as provided in, but subject to all limitations and requirements set forth in, the CRC License.

jove JOURNAL OF VISUALIZED EXPERIMENTS
1 Alewife Center #200
Cambridge, MA 02140
tel. 617.945.9051
www.jove.com

ARTICLE AND VIDEO LICENSE AGREEMENT

4. **Retention of Rights in Article.** Notwithstanding the exclusive license granted to JoVE in **Section 3** above, the Author shall, with respect to the Article, retain the non-exclusive right to use all or part of the Article for the non-commercial purpose of giving lectures, presentations or teaching classes, and to post a copy of the Article on the Institution's website or the Author's personal website, in each case provided that a link to the Article on the JoVE website is provided and notice of JoVE's copyright in the Article is included. All non-copyright intellectual property rights in and to the Article, such as patent rights, shall remain with the Author.

5. **Grant of Rights in Video – Standard Access.** This **Section 5** applies if the "Standard Access" box has been checked in **Item 1** above or if no box has been checked in **Item 1** above. In consideration of JoVE agreeing to produce, display or otherwise assist with the Video, the Author hereby acknowledges and agrees that, Subject to **Section 7** below, JoVE is and shall be the sole and exclusive owner of all rights of any nature, including, without limitation, all copyrights, in and to the Video. To the extent that, by law, the Author is deemed, now or at any time in the future, to have any rights of any nature in or to the Video, the Author hereby disclaims all such rights and transfers all such rights to JoVE.

6. **Grant of Rights in Video – Open Access.** This **Section 6** applies only if the "Open Access" box has been checked in **Item 1** above. In consideration of JoVE agreeing to produce, display or otherwise assist with the Video, the Author hereby grants to JoVE, subject to **Section 7** below, the exclusive, royalty-free, perpetual (for the full term of copyright in the Article, including any extensions thereto) license (a) to publish, reproduce, distribute, display and store the Video in all forms, formats and media whether now known or hereafter developed (including without limitation in print, digital and electronic form) throughout the world, (b) to translate the Video into other languages, create adaptations, summaries or extracts of the Video or other Derivative Works or Collective Works based on all or any portion of the Video and exercise all of the rights set forth in (a) above in such translations, adaptations, summaries, extracts, Derivative Works or Collective Works and (c) to license others to do any or all of the above. The foregoing rights may be exercised in all media and formats, whether now known or hereafter devised, and include the right to make such modifications as are technically necessary to exercise the rights in other media and formats. For any Video to which this **Section 6** is applicable, JoVE and the Author hereby grant to the public all such rights in the Video as provided in, but subject to all limitations and requirements set forth in, the CRC License.

7. **Government Employees.** If the Author is a United States government employee and the Article was prepared in the course of his or her duties as a United States government employee, as indicated in **Item 2** above, and any of the licenses or grants granted by the Author hereunder exceed the scope of the 17 U.S.C. 403, then the rights granted hereunder shall be limited to the maximum rights permitted under such statute. In such case, all provisions contained herein that are not in conflict with such statute shall remain in full force and effect, and all provisions contained herein that do so conflict shall be deemed to be amended so as to provide to JoVE the maximum rights permissible within such statute.

8. **Protection of the Work.** The Author(s) authorize JoVE to take steps in the Author(s) name and on their behalf if JoVE believes some third party could be infringing or might infringe the copyright of either the Author's Article and/or Video.

9. **Likeness, Privacy, Personality.** The Author hereby grants JoVE the right to use the Author's name, voice, likeness, picture, photograph, image, biography and performance in any way, commercial or otherwise, in connection with the Materials and the sale, promotion and distribution thereof. The Author hereby waives any and all rights he or she may have, relating to his or her appearance in the Video or otherwise relating to the Materials, under all applicable privacy, likeness, personality or similar laws.

10. **Author Warranties.** The Author represents and warrants that the Article is original, that it has not been published, that the copyright interest is owned by the Author (or, if more than one author is listed at the beginning of this Agreement, by such authors collectively) and has not been assigned, licensed, or otherwise transferred to any other party. The Author represents and warrants that the author(s) listed at the top of this Agreement are the only authors of the Materials. If more than one author is listed at the top of this Agreement and if any such author has not entered into a separate Article and Video License Agreement with JoVE relating to the Materials, the Author represents and warrants that the Author has been authorized by each of the other such authors to execute this Agreement on his or her behalf and to bind him or her with respect to the terms of this Agreement as if each of them had been a party hereto as an Author. The Author warrants that the use, reproduction, distribution, public or private performance or display, and/or modification of all or any portion of the Materials does not and will not violate, infringe and/or misappropriate the patent, trademark, intellectual property or other rights of any third party. The Author represents and warrants that it has and will continue to comply with all government, institutional and other regulations, including, without limitation all institutional, laboratory, hospital, ethical, human and animal treatment, privacy, and all other rules, regulations, laws, procedures or guidelines, applicable to the Materials, and that all research involving human and animal subjects has been approved by the Author's relevant institutional review board.

11. **JoVE Discretion.** If the Author requests the assistance of JoVE in producing the Video in the Author's facility, the Author shall ensure that the presence of JoVE employees, agents or independent contractors is in accordance with the relevant regulations of the Author's institution. If more than one author is listed at the beginning of this Agreement, JoVE may, in its sole

jove JOURNAL OF VISUALIZED EXPERIMENTS
1 Alewife Center #200
Cambridge, MA 02140
tel. 617.945.9051
www.jove.com

ARTICLE AND VIDEO LICENSE AGREEMENT

discretion, elect not take any action with respect to the Article until such time as it has received complete, executed Article and Video License Agreements from each such author. JoVE reserves the right, in its absolute and sole discretion and without giving any reason therefore, to accept or decline any work submitted to JoVE. JoVE and its employees, agents and independent contractors shall have full, unfettered access to the facilities of the Author or of the Author's institution as necessary to make the Video, whether actually published or not. JoVE has sole discretion as to the method of making and publishing the Materials, including, without limitation, to all decisions regarding editing, lighting, filming, timing of publication, if any, length, quality, content and the like.

12. **Indemnification.** The Author agrees to indemnify JoVE and/or its successors and assigns from and against any and all claims, costs, and expenses, including attorney's fees, arising out of any breach of any warranty or other representations contained herein. The Author further agrees to indemnify and hold harmless JoVE from and against any and all claims, costs, and expenses, including attorney's fees, resulting from the breach by the Author of any representation or warranty contained herein or from allegations or instances of violation of intellectual property rights, damage to the Author's or the Author's institution's facilities, fraud, libel, defamation, research, equipment, experiments, property damage, personal injury, violations of institutional, laboratory, hospital, ethical, human and animal treatment, privacy or other rules, regulations, laws, procedures or guidelines, liabilities and other losses or damages related in any way to the submission of work to JoVE, making of videos by JoVE, or publication in JoVE or elsewhere by JoVE. The Author shall be responsible for, and shall hold JoVE harmless from, damages caused by lack of sterilization, lack of cleanliness or by contamination due to the making of a video by JoVE its employees, agents or independent contractors. All sterilization, cleanliness or decontamination procedures shall be solely the responsibility of the Author and shall be undertaken at the Author's expense. All indemnifications provided herein shall include JoVE's attorney's fees and costs related to said losses or damages. Such indemnification and holding harmless shall include such losses or damages incurred by, or in connection with, acts or omissions of JoVE, its employees, agents or independent contractors.

13. **Fees.** To cover the cost incurred for publication, JoVE must receive payment before production and publication of the Materials. Payment is due in 21 days of invoice. Should the Materials not be published due to an editorial or production decision, these funds will be returned to the Author. Withdrawal by the Author of any submitted Materials after final peer review approval will result in a US$1,200 fee to cover pre-production expenses incurred by JoVE. If payment is not received by the completion of filming, production and publication of the Materials will be suspended until payment is received.

14. **Transfer, Governing Law.** This Agreement may be assigned by JoVE and shall inure to the benefits of any of JoVE's successors and assignees. This Agreement shall be governed and construed by the internal laws of the Commonwealth of Massachusetts without giving effect to any conflict of law provision thereunder. This Agreement may be executed in counterparts, each of which shall be deemed an original, but all of which together shall be deemed to me one and the same agreement. A signed copy of this Agreement delivered by facsimile, e-mail or other means of electronic transmission shall be deemed to have the same legal effect as delivery of an original signed copy of this Agreement.

A signed copy of this document must be sent with all new submissions. Only one Agreement is required per submission.

CORRESPONDING AUTHOR

Name:	Ke Liu and Shusheng Gong
Department:	Department of Otolaryngology Head and Neck Surgery
Institution:	Beijing Friendship Hospital, Capital Medical University
Title:	Morphological and functional Evaluation of Ribbon Synapse at specific frequency Region of the mouse cochlea
Signature:	[signature]
Date:	30th, September, 2018

Please submit a **signed** and **dated** copy of this license by one of the following three methods:

1. Upload an electronic version on the JoVE submission site
2. Fax the document to +1.866.381.2236
3. Mail the document to JoVE / Attn: JoVE Editorial / 1 Alewife Center #200 / Cambridge, MA 02140

Jan 3, 2019, Beijing

Alisha DSouza
Senior Review Editor
Journal of Visualized Experiments

Dear Dr. Alisha DSouza,

Thank you very much for your thoughtful review and consideration of our manuscript entitled "*Morphological and Functional Evaluation of Ribbon Synapses at Specific Frequency Regions of the Mouse Cochlea* (59189 _R1)" for publication in the *Journal of Visualized Experiments*.

In accordance with the comments and suggestions of the editor, which have helped us to substantially improve the quality of our manuscript, we have revised the text in preparation for resubmission as requested. In the revised manuscript, we have incorporated our responses to the editor, which are appended at the end of this letter. We believe that our responses have adequately addressed all editorial concerns and hope that our revised manuscript is now suitable for publication in your esteemed journal.

Additionally, we made a change in the order of the corresponding authors in the author list of the article, which is in accordance with the requests and contributions of the corresponding authors. And all other authors have agreed with this change.

Please feel free to respond with any further questions or concerns. Thank you again for your assistance during the editorial process, and we look forward to your response.

Sincerely,

Ke Liu
Department of Otolaryngology, Head and Neck Surgery, Beijing Friendship Hospital, Capital Medical University
Beijing, P. R. China
Tel: +86 13811488642
E-mail: Keliu66@hotmail.com

Replies to Editorial Comments

Please see the attached word document. In-text comments have been made; these require your attention. Please address the comments by editing your manuscript/figures. Please maintain the current format and track all your edits.

Response: We have revised the manuscript in accordance with the comments and suggestions. We have addressed each of the editorial comments individually, which are appended at the end of this letter.

-Line 167: I restructured this for clarity. How exactly is this fit in? is it simply place in the ear canal? How is it secured?

Response: The tip is cone-shaped, which can be tightly fitted into the external ear canal with its entrance. There is no space to move for the tip, therefore it is secured.

-Line 184: Reference fig 1 here?

Response: We have referenced fig 1 here.

-Line 197: Mention surgical tools used.

Response: The relevant information has been included as follows: “Using a fine forceps, remove the temporal bones, sever the stapes artery, remove the stapes from the oval window, and rupture the round window membrane.”

-Line 199: What size?

Response: The relevant information has been included as follows: “Make a small hole at the apex of the cochlea by gently rotating the tip of the needle (13 mm, 27 G).”

-Line 225: Citing a reference is not sufficient for filming. Please mention dissection steps involved. Mention surgical tools used.

Response: The relevant information has been included as follows: “Use #3, #5 Dumont forceps and the 27 G needle to dissect the apical, middle and basal cochlear regions in turn and then dissect the cochlea out of the bone under a stereo dissection microscope, as previously described.”

-Line 226: Cut how? Mention surgical tools used. Please size of the cut.

Response: The relevant information has been included as follows: “Make a series of small cuts along the spiral ligament using a razor blade , and remove the tectorial membrane and Reissner’s membrane.”

-Line 238: Nothing to film here so I am unhighlighting this.

Response: In accordance with your recommendation, the text has been unhighlighted.

-Line 242: Nothing to film here so I am unhighlighting this.

Response: In accordance with your recommendation, the text has been unhighlighted.

-Line 246: Nothing to film here so I am unhighlighting this.

Response: In accordance with your recommendation, the text has been unhighlighted.

-Line 246: Can you provide the conversion formula here for completeness? If so, we could then include this step for filming and show the formula in the video.

Response: The conversion formula has been included as follows: "d(%) = 1 - 156.5 + 82.5 × log(f), with a slope of 1.25 mm/octave of frequency, where *d* is the normalized distance from the cochlear apex in percent, *f* is the frequency in kHz."

-Line 248: Reference fig 2 here?

Response: We have referenced fig 2 at step 3.5.

-Line 255: The goat serum with TX100?

Response: Yes, the blocking/permeabilization solution is 10% goat serum/PBS/0.1% Triton X-100.

-Line 291: Excitation?

Response: The text has been corrected.

-Line 292: Excitation?

Response: The text has been corrected.

-Line 293: Excitation?

Response: The text has been corrected.

-Line 295: Mention stack height?

Response: The relevant information has been included as follows: "Acquire confocal z-stacks over a distance of 8 μm from each cochlear turn using a 63x high-resolution oil immersion lens."

-Line 304: Is this done in image processing software? Please mention all button clicks and selections in explicit detail.

Response: The number of synaptic puncta for each IHC is calculated manually. The image processing software is only used for the counting of total synaptic puncta at specific frequency regions.

-Line 304: This is a bit vague. Please clarify the steps.

Response: We apologize for the lack of clarity in the original text, which has been revised as follows: "Divide synaptic counts in each z-stack at specific frequency regions by the number of IHCs (equal to the DAPI nuclear manual counts) to calculate the number of synaptic puncta for each IHC."

-Line 305: Is the counting done manually? It appears that the counting is described below, is that correct?

Response: The DAPI nuclear count is performed manually, which is equal to the number of IHCs. The counting of total synaptic puncta is performed by image processing software, which is described in the 5.5.1 and 5.5.2. The text has been revised as follows: "Divide synaptic counts in each z-stack at specific frequency regions by the number of IHCs (equal to the DAPI nuclear manual counts) to calculate the number of synaptic puncta for each IHC."

-Line 308: I made this substeps instead of a note and rewrote in the imperative voice. I think it should be moved up before 5.4. Please check and clarify.

Response: We have checked the substep carefully and moved it up at 5.4. The description of "Experimenters should remain blinded as to whether the slide is from the apex, middle, or basal turn of the cochlea" should be considered as a note.

-Line 313: Reference fig 3 here?

Response: We have referenced fig 3 at step 5.7.

-Line 319: Set to what levels? Please mention all button clicks and selections in explicit detail.

Response: The relevant information has been included as follows: “To visually assess synaptic structure and distribution, we used Photoshop (Adobe) to manually isolate individual IHCs from their neighbors by the Brush Tool to better visualize the cytoskeletal architecture and synaptic localization.”

-*Line 320: How? Please mention all button clicks and selections in explicit detail. This needs more details.*

Response: The relevant information has been included as follows: “To visually assess synaptic structure and distribution, we used Photoshop (Adobe) to manually isolate individual IHCs from their neighbors by the Brush Tool to better visualize the cytoskeletal architecture and synaptic localization.”

-*Line 323: Please mention all button clicks and selections in explicit detail. Unclear what is being done here, so we cannot film as written.*

Response: The relevant information has been included as follows: “To inspect the juxtaposition of presynaptic ribbons (CtBP2) and postsynaptic receptor patches (GluR2), we used Photoshop extracts the voxel space around ribbon by the Rectangular Marquee Tool and isolate individual ribbon by Image Cutting.”

-*Line 325: Please mention all button clicks and selections in explicit detail.*

Response: The relevant information has been included as follows: “Through clicking Image > Image Size, acquire a thumbnail array of these miniature

projections, which can then be used to identify paired synapses (appeared as closely juxtaposed pairs of CtBP2-positive and GluR2-positive puncta) versus orphan ribbons (lacking postsynaptic glutamate receptor patches).”

-Line 326: Unclear how you define paired synapses and orphan ribbons. Please clarify and all the necessary details.

Response: The relevant information has been included as follows: “Through clicking Image > Image Size, acquire a thumbnail array of these miniature projections, which can then be used to identify paired synapses (appeared as closely juxtaposed pairs of CtBP2-positive and GluR2-positive puncta) versus orphan ribbons (lacking postsynaptic glutamate receptor patches).”

-Line 348: There is nothing to film here unless you describe some actions to perform. I have unhighlighted this section.

Response: In accordance with your recommendation, the text has been unhighlighted.

-Line 350: Define P1 and N1.

Response: The relevant information has been included as follows: “ABR wave I amplitude is defined as the difference in voltage between Ip (the positive peak of wave I) and In (the negative peak of wave I).”

-Line 350: Reference fig 4 here?

Response: We have referenced fig 4 here.